Case Report

Necrotic lung tumor mimicking primary pulmonary abscess on computed tomographic imaging study in a dyspneic dog

Mihyun Choi[1] Namsoon Lee[2*]

Abstract

A 14-year-old spayed female Shih-Tzu dog was evaluated for a 1-month history of progressive coughing. Results of the complete blood count and serum biochemistry panel indicated inflammation. Thoracic radiography showed pleural effusion, and cytology revealed septic pyothorax. After antibiotics medication, the patient improved clinical signs but relapsed pleural effusion with a suspicious lung lesion. Computed tomography (CT) of the thorax showed a cavitary lesion with ring-enhanced irregular walls and poorly defined margins in the left cranial lung lobe. The main differential diagnosis considered was lung abscess, but the histopathological diagnosis was necrotic lung adenocarcinoma. This case suggests that both a necrotic lung tumor and a lung abscess are differential diagnoses for ring-enhancing lesions on contrast-enhanced CT images. Especially in the case of septic pyothorax that does not improve or relapse with medical treatment, the underlying cause of a primary lung neoplasm should be suspected.

Keywords: computed tomography, dog, lung abscess, necrotic lung tumor

[1]*BON Animal Medical Center, Korea*
[2]*Section of Medical Imaging, Veterinary Medical Center, Chungbuk National University, Cheongju 28644, Korea*
****Correspondence**: ultravet@cbnu.ac.kr* (N. Lee)
Received: March 3, 2024
Accepted: August 8, 2024

Introduction

A lung abscess is a localized area in the lungs where tissue necrosis has occurred, leading to the formation of a cavity filled with pus or fluid. This condition is typically caused by a bacterial infection and can lead to significant destruction of lung tissue (Bartlett and Gorbach, 1975). In human medicine, lung abscesses are classified as primary or secondary. Primary lung abscesses occur in otherwise healthy individuals due to direct infection of the lung parenchyma, whereas secondary lung abscesses result from underlying conditions such as endobronchial obstructing lung cancer (Kuhajda *et al*., 2015).

In the veterinary literature, reports of pulmonary abscesses are relatively rare, with documented cases in a limited number of cats and dogs (Crisp *et al*., 1987; Hesselink and van den Tweel, 1990; Hylands, 2006; Leighton and Olson, 1967; Nishi *et al*., 2022; Robinson *et al*., 2003; Walker and Nakamura, 2014). The causes in these cases often remain undetermined, though pneumonia or foreign body migration are suspected in most cases (Walker and Nakamura, 2014; Hylands, 2006).

To our knowledge, there are no published cases describing secondary lung abscesses due to necrotic lung tumors, and the initial problem was septic pyothorax in dogs. This case report aims to describe the clinical manifestation and imaging characteristics, emphasizing the similarity of these conditions and their diagnostic challenges.

Case description

A 14-year-old, spayed female Shih-Tzu, weighing 4.7 kg, presented with a 1-month history of progressive coughing after being administered a bronchodilator at the referring veterinary hospital for treatment of tracheal and bronchial collapse. Tachypnea was observed on physical examination. A complete blood count showed leukocytosis. Serum biochemistry revealed elevated alkaline phosphatase, aspartate transferase, and C-reactive protein (Table 1).

Thoracic radiography (Figure 1A) revealed a large amount of pleural effusion. Fluid analysis confirmed exudate (Table 1) with a large number of degenerated neutrophils with phagocytized rods and positive culture result at the blood agar, leading to a diagnosis of septic pyothorax. Antibiotics sensitivity test was not performed due to owner's financial constraints, so we initially administered amoxicillin-clavulanic acid (15 mg/kg, p.o.; Amocla Tab. 375mg, Khunil, Korea) and enrofloxacin (6 mg/kg, p.o.; ASHIENRO 50, ASHISH LIFE SCIENCE PVT. LTD, India), and subsequent radiographic monitoring showed a gradual decrease in pleural effusion and normalized CRP value as well as improved clinical signs. Although the left lung lobe showed soft tissue opacity, the lesion was suspected to represent a lung silhouette sign due to the remaining pleural effusion (Figure 1B). After 1 month, the patient presented with recurrent severe coughing, and a homogeneous mass-like lesion in the left thoracic cavity, without pleural effusion, was confirmed on thoracic radiography. The lesion appeared as an anechoic cystic structure on ultrasonography, so it was aspirated for cytologic examination. In the smear, degenerated neutrophils were found, and no neoplastic disease was observed. To acquire detailed information about the lesion, a computed tomographic (CT) examination was performed. The patient was pre-medicated with butorphanol (0.2 mg/kg, i.v.; Butophan Inj. 1mg/mL, Myung Moon, Korea), anesthetized with propofol (6 mg/kg, i.v.; Provive Inj. 1%, Pharmbio Korea, Korea), maintained with isoflurane (Ifran, Hana Pharm. Co., Korea) supplied with oxygen, and positioned in ventral recumbency through a 16-slice CT scanner (Activion 16, Toshiba Medical Systems, Tochigi, Japan). Thoracic CT images were acquired before and after intravenous injection of iohexol (Omnipaque™ 300, GE Healthcare, IL, USA), which was administered at a dose of 700 mg/kg, using a power injector (LF CT 9000 ADV, Liebel-Flarsheim, USA) at an injection rate of 2.5 m/sec. The breath-hold technique was performed by inducing apnea with manual ventilation. The CT protocol was as follows: 1.0-mm slice thickness, 120 kVp, 150 mAs, 512 × 512 matrix, and 0.75 s/rotation. The images were reconstructed in a 2.0 mm transverse sequence, with sagittal and dorsal reformatted imaging using soft tissue and lung algorithms. A multi-lobular septate thin wall structure, approximately 3.3 × 4.5 × 7.6 cm, containing homogeneous non-contrast enhanced fluid (50 Hounsfield unit [HU]) and small gas cap in the overall left cranial lung lobe (Figure 2A, B, and C). The lobar bronchus in the left cranial lung lobe abruptly terminated. The lung lobe showed peripheral ring-enhanced and poorly defined margins (Figures 2D, E, and F). Additionally, a space-occupying, high attenuating lesion (74 HU) without contrast enhancement (1.5 cm height, 19 cm width, 2.4 cm length) was present in the left cranial lung lobe (Figure 2B and E). The heart deviated to the right due to the enlarged left cranial lung lobe. Mild ground-glass opacities were observed in the right cranial lung lobe, with marginal consolidation. There was a small volume of pleural effusion with pleural thickening but no lymphadenopathy. A left cranial lung lobe abscess within a blood clot was tentatively diagnosed based on the peripheral ring-enhanced, cystic-like structure combined with previously septic pyothorax and a highly attenuating lesion on pre-contrast CT imaging. Although leakage of the lung abscess was considered stopped, there was no response to medical treatment, and surgical resection was planned.

During the median sternotomy, a large mucinous fluid-filled structure adhering to the chest wall was identified. This structure was connected to the caudal part of the cranial lung lobe, necessitating the resection of the entire left cranial lung lobe. (Figure 3A and B). No other abnormal structures or pathological findings were observed in the thoracic cavity. The suctioned fluid from the lesion contained degenerated neutrophils, but negative cultures resulted in the blood agar. The patient recovered and was discharged after 9 days. At that time, there were no remarkable findings in the other lung parenchyma on the thoracic radiographs (Figure 4A).

Histopathological examination (Antech Diagnostics, USA) of hematoxylin and eosin-stained sections (Figure 3C) of the left cranial lung lobe revealed a variably dense fibrovascular stroma with

foci of hemorrhage, necrosis and scattered mild to moderate infiltrates of neutrophils, eosinophils and macrophages around large irregular bronchiolar structures lined by ciliated columnar epithelium with mucus laden goblet cells. In the fibrous stroma around the presumed bronchiolar structures, there were focal tubulopapillary proliferations of cuboidal epithelium. The normal alveolar structure was rarely seen with extensive lymphatic invasion. Based on the histopathological findings, pulmonary adenocarcinoma was diagnosed.

Because the owner refused further treatment, no chemotherapy was administered. Two months later, the patient was evaluated again for tachypnea, and multiple pulmonary miliary nodules with pleural effusion were confirmed on radiographs (Figure 4B). The dog was treated with furosemide (1 mg/kg, p.o.; Lasix Tab. 40 mg, Handok, Korea), and repeated thoracocentesis was performed to maintain patient comfort. After 3 months, the patient was lost to follow-up.

Table 1 Results of blood and fluid analysis of thoracocentesis.

Blood analysis			
	Measurement	**Value**	**Reference interval**
CBC	White blood count (10^3/L)	19.1	6-12
	Hemoglobin (g/dL)	12.8	15-20
	Platelet (10^9/L)	507	200-460
	Hematocrit (%)	37.1	44-57
Serum Chemistry	Alanine aminotransferase (U/L)	76	17-78
	Aspartate transferase (U/L)	48	17-44
	Alkaline phosphatase (U/L)	601	47-254
	Gamma Glutamyl Transferase (U/L)	9	5-14
	Blood urea nitrogen (mg/dL)	9.8	9.2-29.2
	Creatinine (mg/dL)	0.36	0.4-1.4
	Calcium (mg/dL)	12.4	9.3-12.1
	Phosphorus (mg/dL)	3.7	1.9-5
	Total protein (g/dL)	6.3	5-7.2
	Albumin (g/dL)	2.9	2.6-4
	Total bilirubin (mg/dL)	0.3	0.1-0.5
	Glucose (mg/dL)	104	75-128
	C-reactive protein (mg/L)	135	1-9
Fluid analysis			
Thoracocentesis	Total protein (g/dL)	6.2	-
	Total nucleated cell count (μL)	71300	-

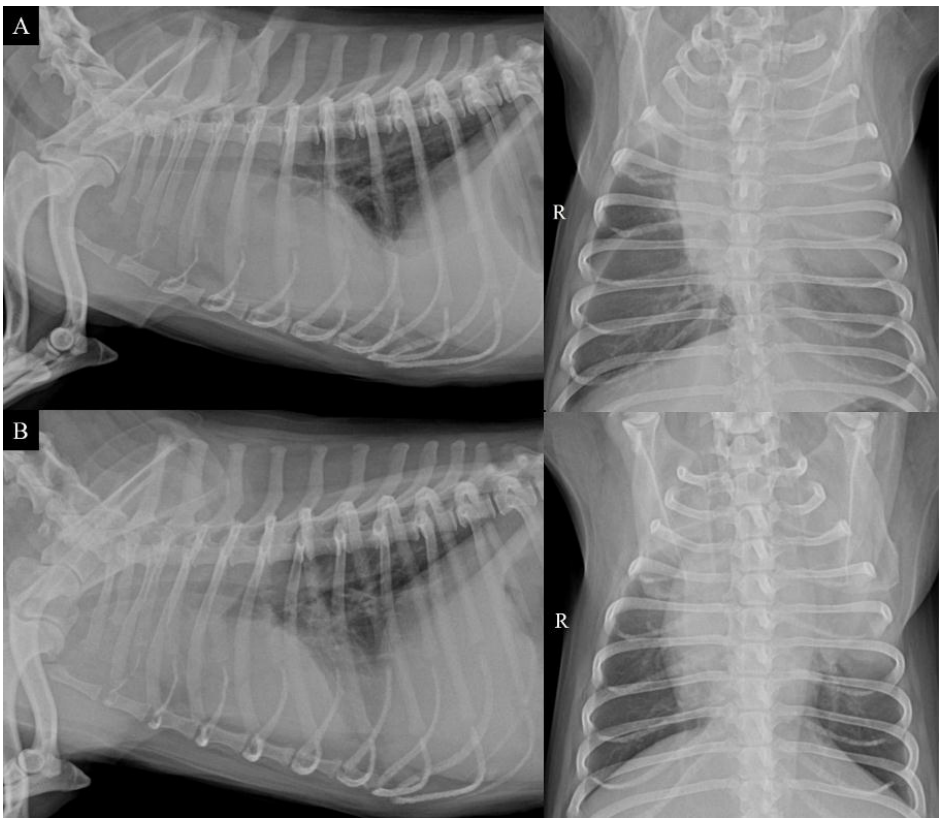

Figure 1 Right lateral (left side) and ventrodorsal (right side) radiographs (A, day 0 and B, day 3). A large amount of pleural effusion was identified and diagnosed as septic pyothorax (A). A decreased amount of pleural effusion was identified, along with a mild increase in left cranial lung opacity (B).

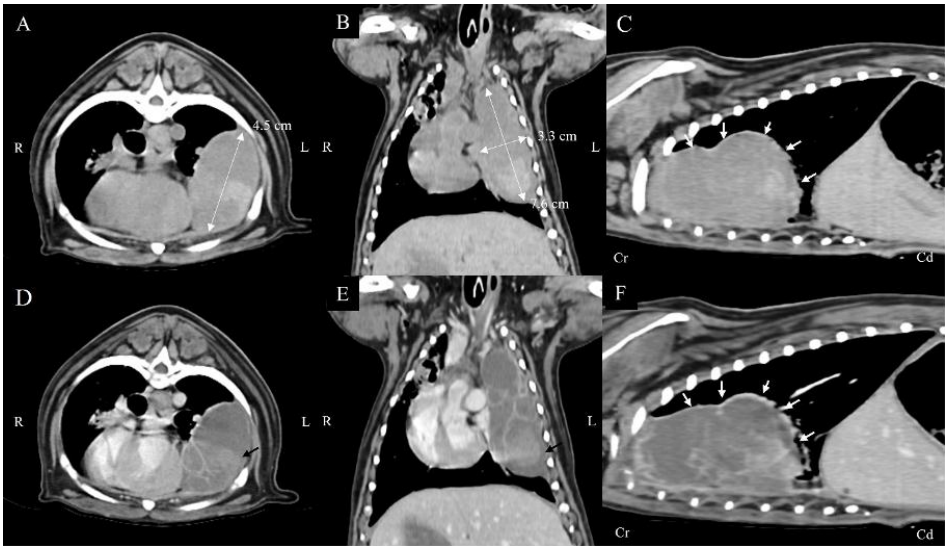

Figure 2 Pre (A, B and C) and pos-contrast (D, E and F) thoracic CT reconstructed images displayed in the soft tissue window. There was a high attenuating material (black arrows) with no contrast enhancement within the left cranial lung lobe (D and E). The left cranial lung lobe (white arrows) identified a fluid-filled structure with rim enhancement (C and F).

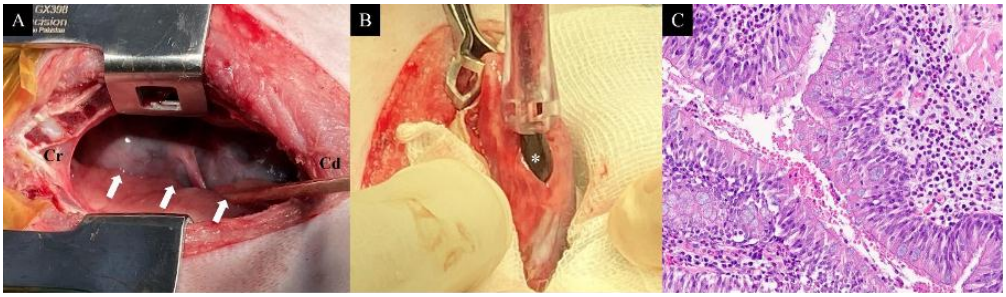

Figure 3 Intraoperative surgical images of the left cranial lung lobe (A and B) and histopathology of the left cranial lung lobe (C). A large fluid-filled structure (A, arrows) adhered to the chest wall, and dark brown fluid was suctioned from the structure (B, asterisk). Variable dense fibrovascular stroma with foci of hemorrhage, necrosis, and scattered mild to moderate infiltrates of inflammatory cells around large irregular bronchiolar structures, which have replaced the left cranial lung lobe. There was vascular ectasia neovascularization with extensive lymphatic invasion (C, HE stain, X 400).

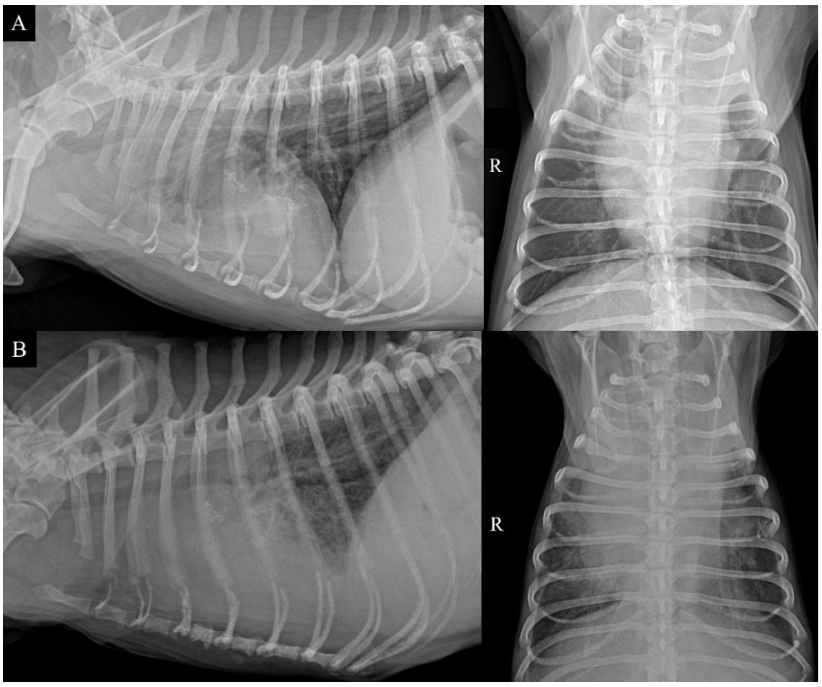

Figure 4 Right lateral (left side) and ventrodoral radiographs (right side). After the left cranial lung lobectomy, other lung parenchyma showed normal (A). Two months later, comparing previous postoperative thoracic radiographs, multiple lung miliary nodules with pleural effusion were confirmed on radiographs (B).

Results and Discussion

In the present case, during the initial examination, the patient responded effectively to antibiotic medication, suggesting that the likely cause of the septic pyothorax was pneumonia. Additionally, the size of the primary lung lesion was initially reduced, which led us not to be concerned about other causes at that time. However, within one month, the primary lung lesion increased in size again, showing cystic changes. The left lung lobe was replaced by a thin-walled round hypodense area with peripheral contrast enhancement observed in CT images, leading to a tentative diagnosis of chronic pneumonia transforming into a lung abscess. However, histopathological examination ultimately diagnosed the lesion as a malignant necrotic lung tumor rather than pneumonia.

Several theories explain why lung abscesses occur in the presence of malignancy. These include bronchial obstruction and vascular involvement, leading to ischemia and tumor necrosis, followed by suppurative obstructive pneumonia and abscess formation (Kuhajda *et al*., 2015; Valvani *et al*., 2019). Therefore, in cases where there is no response to or relapse of a lung abscess after antibiotics administration, surgical resection and histopathologic examination should be considered.

CT imaging is crucial for evaluating lung abscesses and distinguishing them from other lung lesions. On CT images, abscesses often appear as round hypodense lesions with smooth and peripheral contrast enhancement (Furuya *et al*., 2012), but malignant necrotic lung tumor also shows peripheral contrast enhancement, making differentiation between both lesions challenging. However, in human medicine, necrotic lung cancer shows a significantly higher incidence rate of thick cavitary walls (Woodring *et al*., 1980). According to a previous study, all of the cavitary lesions with a wall thickness of 1 mm or less in the thickest part were benign. Among lesions with wall thickness of 2-4 mm, 5-15 mm, and more than 15 mm, malignancy rates are 14%, 49%, and 95%, respectively (Woodring *et al*., 1980). In our case, the wall thickness was less than 1 mm, so the lesion was initially considered a benign lung abscess; however, histologic examination revealed the lesion to be malignant. The differentiation between lung abscesses and malignant lung tumors poses significant diagnostic challenges due to overlapping clinical and imaging characteristics. Standard CT imaging, while valuable, may not always provide definitive answers, necessitating the use of more advanced diagnostic tools. Emerging technologies such as dual-energy spectrum CT (DESCT) and PET-CT have shown promise in human medicine due to their ability to provide more detailed tissue characterization and metabolic activity. DESCT, by quantifying iodine uptake, can help distinguish between benign and malignant lesions (Li *et al*., 2021), while PET-CT can highlight areas of increased metabolic activity typical of malignancies (Fletcher *et al*., 2008). Introducing these advanced imaging modalities into veterinary practice could significantly enhance diagnostic accuracy, allowing for more precise treatment planning. Furthermore, integrating molecular and genetic profiling of lung lesions could provide insights into the underlying pathophysiology and potential therapeutic targets, paving the way for personalized veterinary oncology (Rodríguez *et al*., 2021)

Treatment approaches vary significantly between lung abscesses and malignant lung tumors. Lung abscesses typically require prolonged antibiotic therapy and, in some cases, surgical drainage. In contrast, malignant tumors may require surgical resection, chemotherapy, or radiation therapy. Accurate differentiation between a lung abscess and a malignant lung tumor is crucial as it significantly influences the treatment strategy and prognosis. Misdiagnosis can lead to inappropriate treatment, delayed intervention, and potentially poorer outcomes. A multidisciplinary approach is essential in managing these complex cases, involving veterinarians, radiologists, and pathologists

In conclusion, distinguishing a primary lung abscess from a necrotic lung tumor can be quite difficult due to their similar clinical features and imaging characteristics. Both lesions display peripheral contrast enhancement on conventional CT images. Additionally, the malignant lung neoplasia led to the development of a lung abscess and septic pyothorax, as seen in our case. Therefore, if the lung abscess does not improve or recurs after antibiotic treatment, it should raise suspicion of an underlying primary lung malignancy. Surgical resection and histologic examination are essential for accurate diagnosis and appropriate management.

Acknowledgments

The authors would like to thank the dog owners for their kind cooperation during the data collection. We thank Editage for the English language editing.

References

Bartlett JG and Gorbach SL 1975. The triple threat of aspiration pneumonia. Chest. 68: 560-566.

Crisp MS, Birchard SJ, Lawrence AE and Fingeroth J 1987. Pulmonary abscess caused by a Mycoplasma sp in a cat. J Am Vet Med Assoc. 191: 340-342.

Fletcher JW, Kymes SM, Gould M, Alazraki N, Coleman RE, Lowe VJ, Marn C, Segall G, Thet LA and Lee K; VA SNAP Cooperative Studies Group 2008. A comparison of the diagnostic accuracy of 18F-FDG PET and CT in the characterization of solitary pulmonary nodules. J Nucl Med. 49: 179-185.

Furuya K, Yasumori K, Takeo S, Sakino I, Uesugi N, Momosaki S and Muranaka T 2012. Lung CT: Part 1, Mimickers of lung cancer--spectrum of CT findings with pathologic correlation. AJR Am J Roentgenol. 199: W454-463.

Hesselink JW and van den Tweel JG 1990. Hypertrophic osteopathy in a dog with a chronic lung abscess. J Am Vet Med Assoc. 196: 760-762.

Hylands R 2006. Veterinary diagnostic imaging. Ruptured lung lobe abscess secondary to a localized alveolar disease. Can Vet J. 47: 181-182.

Kuhajda I, Zarogoulidis K, Tsirgogianni K, Tsavlis D, Kioumis I, Kosmidis C, Tsakiridis K, Mpakas A,

Zarogoulidis P, Zissimopoulos A, Baloukas D and Kuhajda D 2015. Lung abscess-etiology, diagnostic and treatment options. Ann Transl Med. 3: 183.

Leighton RL and Olson S 1967. Hypertrophic osteoarthropathy in a dog with a pulmonary abscess. J Am Vet Med Assoc. 150: 1516-1520.

Li Q, Fan X, Luo TY, Lv FJ and Huang XT 2021. Differentiating malignant and benign necrotic lung lesions using kVp-switching dual-energy spectral computed tomography. BMC Med Imaging. 21: 81.

Nishi R, Ohmi A, Tsuboi M, Yamamoto K and Tomiyasu H 2022. Successful treatment of a lung abscess without surgical intervention in a cat. JFMS Open Rep. 8: 20551169221086434.

Robinson DA, DeNardo GA and Burnside DM 2003. What is your diagnosis? Pulmonary abscess. J Am Vet Med Assoc. 223: 1259-1260.

Rodríguez M, Ajona D, Seijo LM, Sanz J, Valencia K, Corral J, Mesa-Guzmán M, Pío R, Calvo A, Lozano MD, Zulueta JJ and Montuenga LM 2021. Molecular biomarkers in early stage lung cancer. Transl Lung Cancer Res.10: 1165-1185.

Valvani A, Martin A, Devarajan A and Chandy D 2019. Postobstructive pneumonia in lung cancer. Ann Transl Med. 7: 357.

Walker JR and Nakamura RK 2014. What is your diagnosis? Pulmonary abscess. J Am Vet Med Assoc. 245: 277-278.

Woodring JH, Fried AM and Chuang VP 1980. Solitary cavities of the lung: diagnostic implications of cavity wall thickness. AJR Am J Roentgenol. 135: 1269-1271.